Enhancing subsalt imaging through advanced identification and suppression of interbed multiples and mode-converted reflections — Gulf of Mexico and Brazil case studies

Riaz Alai[1], Faqi Liu[2], Eric Verschuur[3], Jan Thorbecke[3], Gundogan Coskun[1], Shuqian Dong[2], Cosmin Macesanu[2], Bin Wang[2], Christopher Lee Slind[1], and Eric Andersen[1]

https://doi.org/10.1190/tle40120905.1

Abstract

In our case studies, the success of subsalt exploration and development wells depended heavily on the characterization of highly heterogeneous lacustrine microbial carbonates. Acoustic and elastic inversions have proved to be a good proxy for identification of reservoir quality variation for exploration and development well placements. However, qualitative and quantitative usage of subsalt seismic amplitudes requires proper illumination and good signal-to-noise ratio. If properly imaged, mode-converted reflections and interbed multiples can be complementary to the P-wave image. But, in conventional P-wave-oriented imaging, both types of events cannot be imaged correctly. They appear as coherent noise and negatively impact the overall exploration and development project outcomes, especially in areas with poor illumination. This paper consists of two parts: first, we investigate the potential problems resulting from converted waves and interbed multiples in data from two different basins — the Gulf of Mexico and the Campos Basin in offshore Brazil — and show our approach to attenuate them to reveal the true structures. The second part focuses on advanced identification of interbed multiples in modeling and migration methods. To facilitate the various strategies to attenuate interbed multiples, "interpretation" of the various events plays a significant role. Vertical seismic profile (VSP) data are excellent for the purpose; however, these data are only available at well locations, if they are recorded. As a result of many years of technology advancement, pseudo VSP data can be constructed effectively from standard streamer survey data. Two methods are highlighted in this paper for building pseudo VSP data in a full two-way sense, based on a typical Brazil-type salt model: Marchenko-based processing and full-wavefield migration. Major subsalt plays in the Gulf of Mexico and emerging plays in Brazil should benefit significantly from elimination of these kinds of coherent noise.

Introduction

Current seismic imaging practices focus on longitudinal (P) waves. In salt-rich settings such as the Gulf of Mexico and offshore Brazil, due to large velocity contrasts between sediments and adjacent salt bodies, strong wave-mode conversions occur between the P-waves and transversal (S) waves. The mode-converted reflections can be recorded during acquisition if they are converted back to P-waves arriving at the hydrophones (Lu et al., 2003; Alai and Verschuur, 2006). These mode-converted waves show up in seismic data as echoes of the P-wave reflections. With the aid of physical modeled data, these effects have been studied in a controlled manner (Alai et al., 2007). Standard imaging for P-wave energy will misposition these converted reflections, making them appear as coherent noise that contaminates the image. Though the converted waves typically are weaker in amplitude, they often can be strong enough to interfere with primary events, especially in areas with poor illumination such as subsalt. In a salt-rich environment such as the Gulf of Mexico (Hegazy et al., 2017) and offshore Brazil, those highly reflecting boundaries may include water bottom and salt boundaries. In the Campos Basin offshore Brazil, carbonate layers above top salt generate strong converted waves contaminating the image at the stratified salt body and the structures underneath. In seismic imaging, mode-converted reflections often make it difficult to identify the base of salt and subsalt structures. This is because of the strong P-wave velocity contrast between salt bodies and adjacent sediment layers, whereas the S-wave velocity within the salt is more comparable with the P-wave velocities within the surrounding sediment layers.

Such complex structures with large impedance contrasts also generate strong interbed multiples. Like mode-converted waves, interbed multiples cannot be properly imaged using conventional prestack depth migration (PSDM). Their interference can mislead the interpretation badly (Wang et al., 2009). Properly attenuating these noise events is crucial to reveal the true structure of the subsurface. Different algorithms have been proposed and applied effectively to attenuate them from the data before migration, especially for interbed multiple removal (Weglein et al., 1997; Jakubowicz, 1998; Griffiths et al., 2011; van der Neut and Wapenaar, 2016; Pereira et al., 2018; Staring and Wapenaar, 2020; Xavier de Melo et al., 2020). However, in case of structural complexity in carbonate or salt bodies, applications of those data domain algorithms remain challenging, partly because they often involve a large amount of data and application of those algorithms may require proper preprocessing, which can be quite time consuming.

A hybrid (data and image) domain workflow has been proven effective to attenuate the unwanted noise from the image. Such

[1]PETRONAS Carigali Sdn. Bhd., Kuala Lumpur, Malaysia. E-mail: riaz.alai@petronas.com; gundogan.coskun@petronas.com; christopher.leeslin@petronas.com; eric.andersen@petronas.com.
[2]TGS, Houston Texas, USA. E-mail: faqi.liu@tgs.com; shuqian.dong@tgs.com; cosmin.macesanu@tgs.com; bin.wang@tgs.com.
[3]Delft University of Technology, Delft, The Netherlands. E-mail: d.j.verschuur@tudelft.nl; j.w.thorbecke@tudelft.nl.

DOI:10.1190/tle40120905.1

a workflow consists of (1) predicting the premigrated data for mode-converted reflections or interbed multiples and (2) prestack imaging of the predicted events followed by (3) adaptive subtraction of the imaged noise events from the original image (Alai and Verschuur, 2003; Lu et al., 2003). This paper showcases the occurrence of these kinds of noise in data from different geologic settings and the application of the workflow to predict and adaptively remove them from the image with the aid of elastic modeling using two data sets: one from the Gulf of Mexico and another from Campos Basin offshore Brazil.

In the second part of this paper, in addition to the removal of interbed multiples as described earlier, interpretation of the various events plays a significant role toward solutions. In particular, for accurate subsalt imaging it is important to track the trajectories of generated interbed multiples and ensure that these are suppressed. For this specific "interpretation," vertical seismic profile (VSP) data are excellent. However, VSP data are not always available and unfortunately are only available at well locations if they are recorded. In the 1990s, the use of so-called pseudo VSP data was advocated (Alai and Wapenaar, 1993). At that time, full two-way processing was difficult without an accurate velocity model. Throughout the years, technology has advanced and more full-waveform approaches have emerged. Two of them are highlighted in this paper: Marchenko-based processing — with Marchenko data redatuming (MDR) and Marchenko multiple elimination (MME) implementations — and full-wavefield migration (FWM). Both MDR and FWM can translate surface measurements into up/downgoing wavefields at any depth (a more detailed description and associated references to follow). In addition, MME can remove interbed multiples, allowing the identification of primaries in the pseudo VSP. In this paper, we showcase the revival of the old concepts of pseudo VSP data generation and the integration with analysis using the Marchenko-based and FWM methodologies.

Estimating/modeling/suppressing interbed multiples and wave-converted reflections

The hybrid domain algorithm has proved to be effective in attenuating the earlier-described coherent noise events (multiples and wave conversions) from a P-wave image. This flow consists of identification, prediction, imaging, and adaptive subtraction of the image of converted reflections or interbed multiples from the original image. As further elaborated in the second part of this paper, Alai and Wapenaar (1993) illustrated the generation of pseudo VSP data as an interpretation tool to identify wave conversions at boundaries and interbed multiples (Alai and Wapenaar, 1994). Their significance varies depending on the geologic setting. Data from offshore Brazil show strong noise events of both kinds related to water bottom, but those are relatively weak in data from the Gulf of Mexico.

Starting with the most accurate subsurface model, the mode-converted waves associated with specific reflectors can be predicted explicitly with a proper velocity model built by adjusting the final P-wave velocity model. For example, to predict the mode-converted waves at the salt-sediment interface, the P-wave velocity within the salt is replaced by the best estimate of the S-wave velocity. Then, to predict an event characterized as PSPP, an arriving P-wave converts to S-wave at the top salt and propagates into the salt body until it is reflected and converted back to P at the base of the salt, which continues to propagate through the salt and top salt (see the event marked by the arrow in Figure 1a). For wavefield propagation, we use a propagator based on a highly accurate one-way wave equation for a tilted transversely isotropic medium (Tang et al., 2019), where downgoing propagation uses the modified velocity, while upgoing propagation uses the original P-wave velocity. Following a similar workflow, by switching between the original P-wave velocity and the newly obtained model, other mode-converted reflections can be predicted correctly, namely, PPSP, PSSP (Figure 1a), or even higher orders of reflections (multiples) such as PSPPSP or PSSPPP. Interbed multiples can be predicted in a similar way, but only P-wave velocity will be used with multiple rounds of propagation for both upgoing and downgoing paths between the multiple generators (Figure 1b).

The properly predicted arrivals can be imaged with the same flow as for the final image using the same P-wave velocity model, which should match with those in the original image, at least in position. They may differ in amplitude, and a curvelet domain filter (Chang et al., 2000; Yang et al., 2020) can be employed to attenuate them adaptively from the original image.

Gulf of Mexico data example

Subsalt imaging in the Gulf of Mexico is challenging, not only because the complex salt geometry often causes significant illumination issues but also because strong mode-converted waves and interbed multiples can be generated at the salt boundaries. Even with an accurate velocity model, the image from subsalt structures can be interfered with strongly or even totally masked by the images of these unwanted wave components, as they can sometimes be relatively strong (Huang et al., 2013).

Figure 2a shows a crossline of a 3D prestack reverse time migration (RTM) image volume, showing a homogeneous salt body with a clearly imaged boundary. However, a noticeably strong event below the salt can be seen roughly tracking the base of salt body. This has been identified as the image of a converted

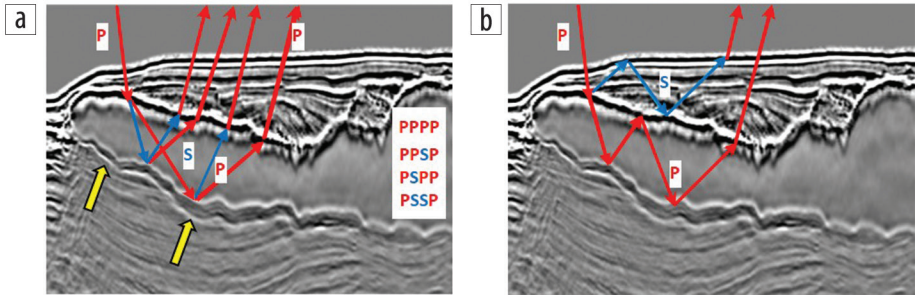

Figure 1. (a) Four different arrivals for a single incident P-wave to the top of salt raypaths of some mode-converted reflections at the salt boundaries. (b) Raypaths of interbed multiples between salt boundaries and water bottom.

DOI:10.1190/tle40120905.1

wave from the salt interface. By replacing the P-wave velocity in salt (Figure 2b) with an S-wave velocity, we predicted the PPSP, PSPP, and PSSP converted waves from the top and bottom salt interfaces using the one-way wave-equation-based propagator. We also predicted the interbed multiple bouncing between the salt interfaces. Their RTM images using the final P-wave velocity are shown in Figure 2c. Clearly these events match kinematically well with the noise events identified in the original image. Note that, despite the presence of the complex salt body, the converted waves at difference lags, PSPP and PPSP, have similar images, and they both have similar structure to the base of salt. An inversion-based adaptive subtraction in curvelet domain successfully attenuates those noisy events from the original image as shown in Figure 2d. Figure 3a shows one inline section of the 3D volume where two salt bodies are close to each other. Converted waves are clearly present in the subsalt area (yellow arrows), and they are attenuated successfully using our prediction and subtraction workflow (Figure 3b).

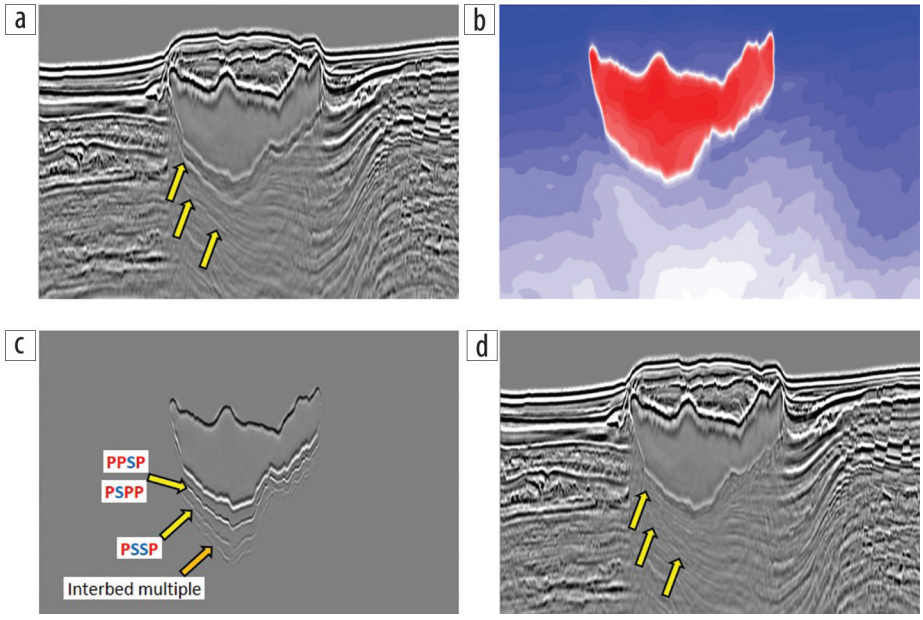

Figure 2. A crossline section in a 3D RTM volume from the Gulf of Mexico: (a) original image, which is contaminated by images of converted wave and interbed multiples; (b) the P velocity model used to build the converted wave velocity model by replacing an S velocity in the salt; (c) image of various predicted converted waves and interbed multiples; and (d) image after adaptively subtracting the noise in (c).

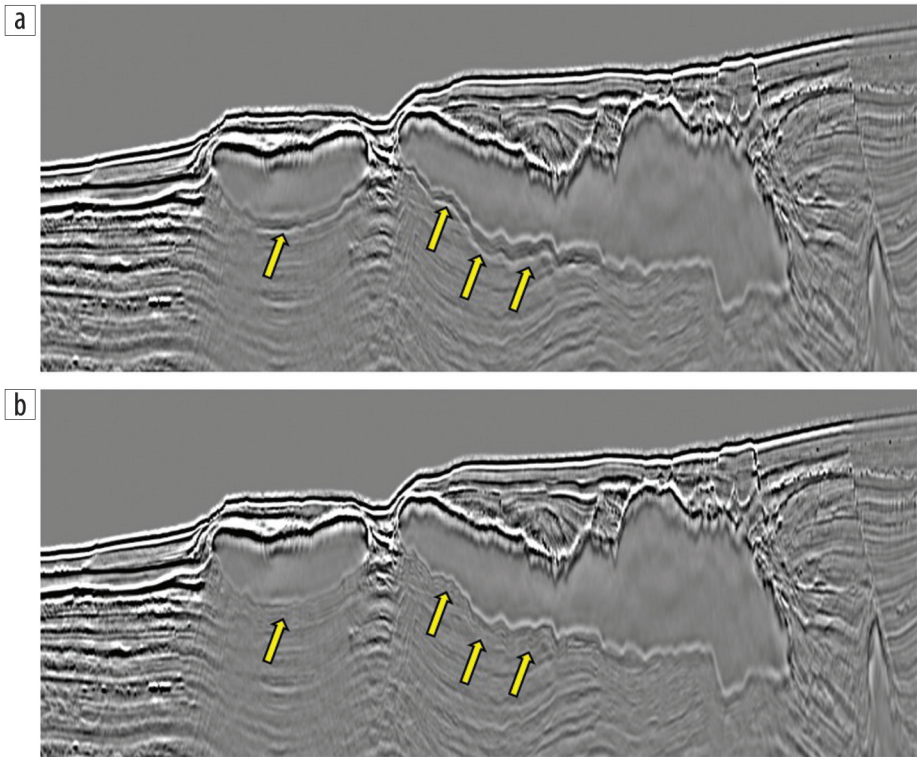

Figure 3. (a) An inline section in the 3D RTM volume from the Gulf of Mexico. (b) Image after adaptively subtracting the images of the predicted converted waves and interbed multiples.

Campos Basin data example, offshore Brazil

Geologic context. Discovery of the giant Tupi/Lula Field by Petrobras in the Santos Basin in 2006 shifted the focus of oil companies to the world-class subsalt play in the deep waters offshore of Brazil. Exploration has achieved an unmatched success ratio reaching 90%–100% in some years, particularly by Brazil's state oil company Petrobras. Subsalt seismic imaging has been key to the identification and successful drilling of highly challenging subsalt opportunities, which had not been identified mainly due to very poor seismic imaging. The subsalt play is extensive, covering both Santos and Campos basins (Figure 4). Large numbers and sizes of discoveries have been made to date, and estimates of yet-to-find reserves are significant, making it still an emerging, competitive play for oil and gas companies (Figure 5).

The play is developed within the rift and transitional sequences of the Santos and Campos basins linked to the opening of the South Central Atlantic initiated in the Lower Cretaceous. The subsalt play is composed of the Barremian-Aptian lacustrine carbonate reservoirs (late synrift coquinas and transitional microbial carbonates) capped/sealed by thick regional Aptian salt. These carbonate reservoirs were charged by world-class oil-prone lacustrine type-I source shales that were deposited in

DOI:10.1190/tle40120905.1

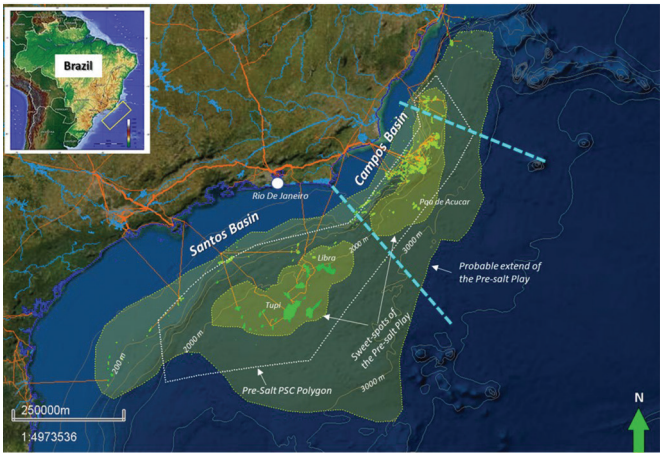

Figure 4. Brazil subsalt play extends across the majority of the Santos and Campos basins with significant running room for exploration mainly lying in the ultra-deep waters.

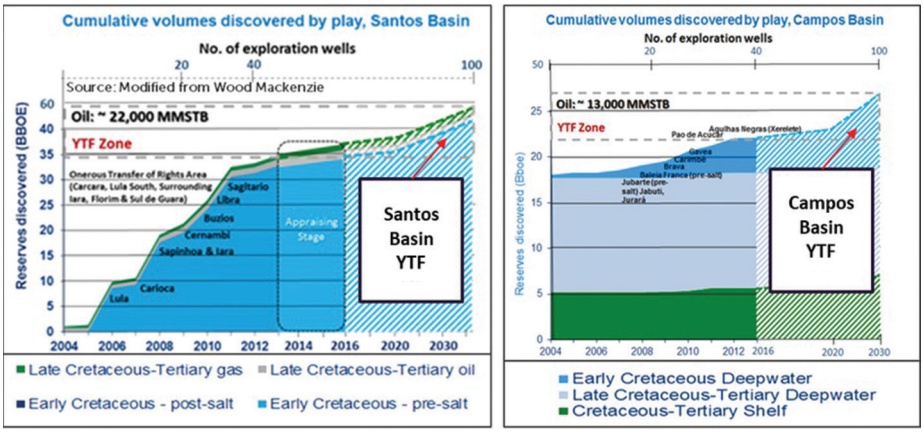

Figure 5. Discovered and yet-to-find volumes of Santos and Campos basins. Note the significant Early Cretaceous subsalt play volumes, especially in the Santos Basin. (Source: Woodmac)

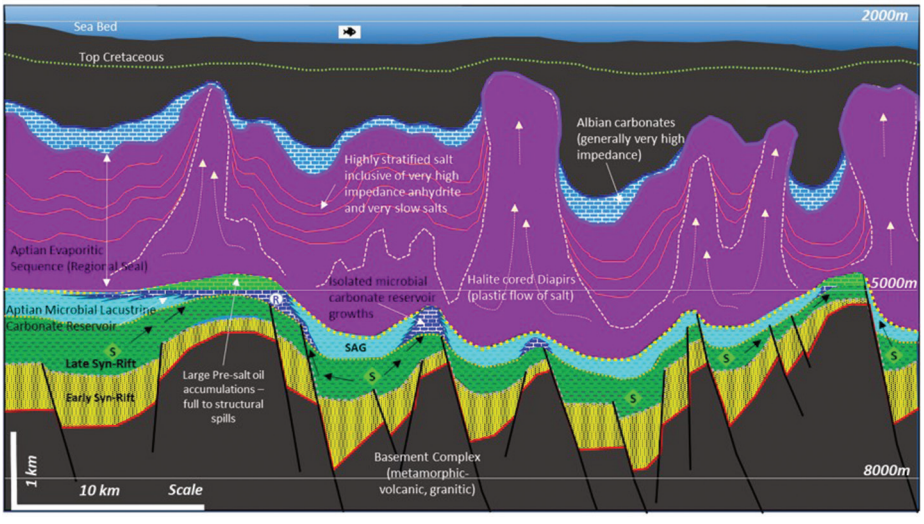

Figure 6. Generalized subsalt play geologic section representative of Brazil subsalt play. Subsalt late synrift lacustrine shales (green section) are mature and rich enough to charge both subsalt and postsalt reservoirs full to spill. Lacustrine microbial carbonates develop over paleo highs (highlighted in blue within the SAG section) and are highly productive (currently averaging 20–25 kbd). The Aptian salt sequence is generally thick and an excellent seal to subsalt structural traps. The salt section may show a high degree of heterogeneity due to its original stratified nature resulting in a very complex seismic overburden to imaging of subsalt reservoirs and sections. The presence of high-velocity Albian carbonates with variable thickness on top of salt creates complex top salt impedance relationship and also creates fair magnitude of subsalt structural distortions.

early synrift, late synrift, and transitional stages (Figure 6). The Brazil subsalt play can be considered as a "Goldilocks" of a petroleum system where all elements are almost perfect — oil-prone prolific source charging the large subsalt as well as postsalt reservoirs full to spill, thick regional salt sealing with infinite sealing capacity, and unmatched deepwater carbonate reservoir productivities reaching as much as 60 kbd per well.

However, the play has its own share of challenges, mainly linked to seismic imaging issues related to its unique salt bodies. In Brazil, the Aptian salt is highly stratified due to cyclicity during the deposition that resulted in various alternating salt layers coupled with anhydrite cycles. There are significant seismic impedance differences between highly stratified layers of this evaporitic sequence. The stratification is more pronounced across the Santos Basin compared to the Campos Basin. The salt halokinesis is a common process that leads to very complex overburden-related imaging problems for subsalt targets. During salt halokinesis, differences in the mechanical behavior of layers (competent anhydrites layers versus plastic salts) result in increased intrasalt geometric and impedance complexity, especially as diapiric areas tend to be halite dominant. The Brazil salt/evaporitic sequence transitions to Albian carbonates, which tend to have dolomites and anhydrite at the lower part. This sequence on top of salt has a very high velocity (5500–6000 m/s) and impedance compared to the salt (4300–4500 m/s) underneath (Figures 7 and 8). Additionally, this sequence can be highly variable in thickness and extent due to salt halokinesis. It generally pinches out against steep flanks of salt diapirs, creating strong lateral velocity variation.

Subsalt exploration offshore Brazil has been shifting to distal stretches where the salt gets much thicker with highly variable and complex geometries resulting in poor subsalt imaging. The problem is further complicated by highly deformed/modified subsalt rift and transitional sequences. As the identification of viable/sizeable structural closures and reservoir facies is essential to highly competitive subsalt, a good seismic imaging becomes crucial to support such exploration programs.

Development reservoir characterization requires delineation of net-to-gross (NTG) and pore volume distribution required for optimum count and placement of development wells. This requires good quality subsalt amplitudes

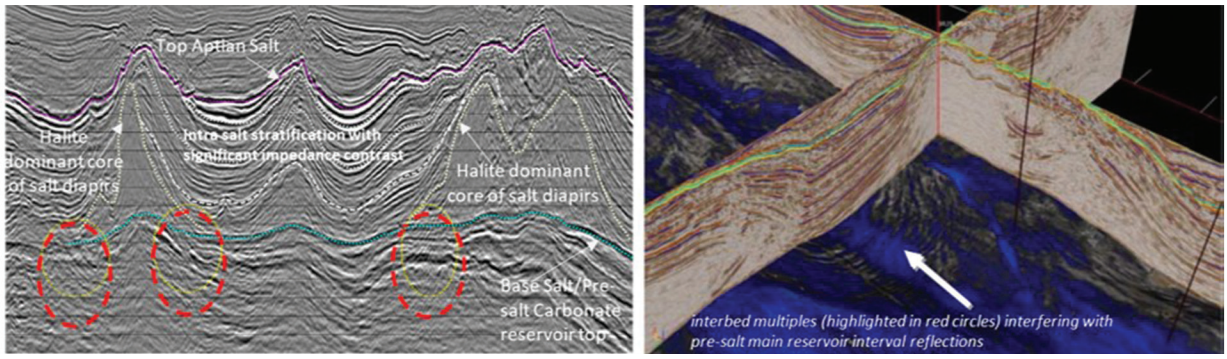

Figure 7. An example of highly stratified salt with significant impedance contrast and different mechanical behavior during salt halokinesis creates interfaces that produce interbed multiples (highlighted in red circles) interfering with subsalt main reservoir interval reflections, from Santos Basin (modified from Penna et al., 2013).

for acoustic and elastic inversions, which seem to correlate well with NTG and pore distribution (reservoir heterogeneity).

There is still a significant range of uncertainty in overall structural shape of subsalt trap leads, volume estimations, and resource distributions. This in turn has significant impact on the overall decisions all the way from highly competitive bidding valuations and drilling of ultra-deepwater exploration wells to development layouts inclusive of development well counts and number and types of floating production, storage, and offloading selections.

Field data example. Figure 9a shows one line of a 3D prestack RTM volume from the Campos Basin offshore Brazil. Unlike in the figures from the Gulf of Mexico (Figures 2 and 3), which have clean salt bodies, coherent events are imaged inside the salt body even though salt interfaces have been imaged nicely. In addition, subsalt structure is contaminated by dipping events (denoted by yellow arrows) cutting through the reflectors, which can be misinterpreted as faults. In fact, they are the images of the converted waves and interbed multiples. However, in contrast to the Gulf of Mexico case, strong conversions in these Campos data take place at top salt and interfaces above it. To confirm this, we generated synthetics from elastic modeling for some shot gathers, using the P-wave and S-wave velocity shown in Figures 10a and 10b, respectively. Figure 10d is a snapshot of the elastic wavefield, clearly showing the shear wave converted at the water bottom and salt boundary, compared to the acoustic snapshot in Figure 10c. Figure 9b is the acoustic RTM image of the P component in elastic data using the P-wave velocity. For comparison, Figure 9c shows the acoustic RTM of acoustically simulated shot gathers at the same shot locations. Figure 9b clearly has many events (see yellow arrows) that are much like those in the real data (Figure 9a), including those in the subsalt area. As expected, they are not present in the image of acoustically modeled data (Figure 9c), indicating these are indeed the images of mode-converted energy. On the other hand, some events exist in the salt body of both Figure 9b and Figure 9c as marked by the orange arrows. These are the images of the interbed multiples associated with the salt and surrounding sediment.

As one can expect, conversion at the deeper part of the salt interface has a more detrimental impact to imaging of the base of the salt and the subsalt structures, where the images of the converted waves interfere with the base of salt and the structures below it. This can be observed clearly in both the field and synthetic

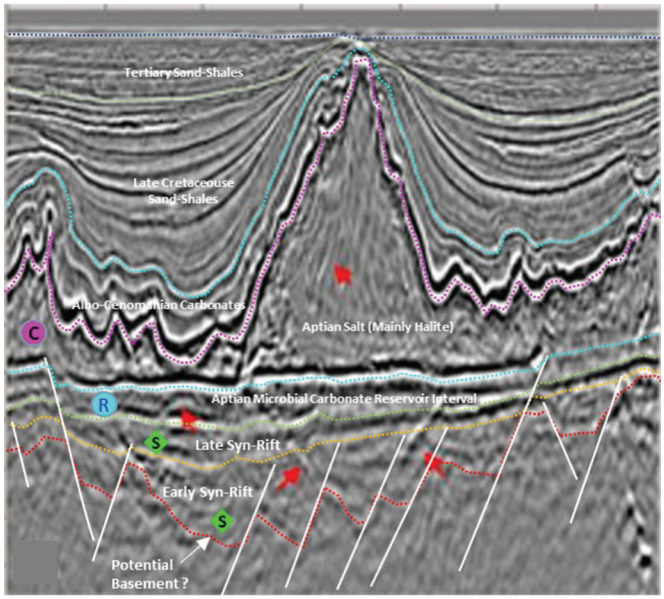

Figure 8. Uncalibrated interpretation highlighting subsalt Aptian reservoir section sealed by Aptian salt, Campos Basin. Note the structural shape of base salt suspiciously following salt thickness/shape variation and presence of noise affecting the interpretation confidence (R: subsalt reservoir, S: subsalt source, C: subsalt play seal).

data. After proper prediction and imaging of the mode-converted reflections associated with strong interfaces between water bottom and base of salt, the contaminating events are properly suppressed from the original image (Figure 9d). Compared with Figure 9a, Figure 9d clearly shows that the strong converted wave events (see yellow arrows) have been well attenuated.

Reviving old concepts with new insights: Pseudo VSP generation through Marchenko methods and FWM

As has been described, an important component to the successful removal of coherent noise events is their identification in the premigrated seismic data. If available, VSP data provide this unique link between the surface observations and the subsurface reflection points. However, because true VSP data are scarce, one can opt for reproducing VSP data from the surface data.

Pseudo VSP data generation. The generation of pseudo VSP data was introduced by Alai and Wapenaar (1993) for elastic waves, and noncausal events were used (as a special criteria) in pseudo VSP data displays to verify the correctness of velocity and

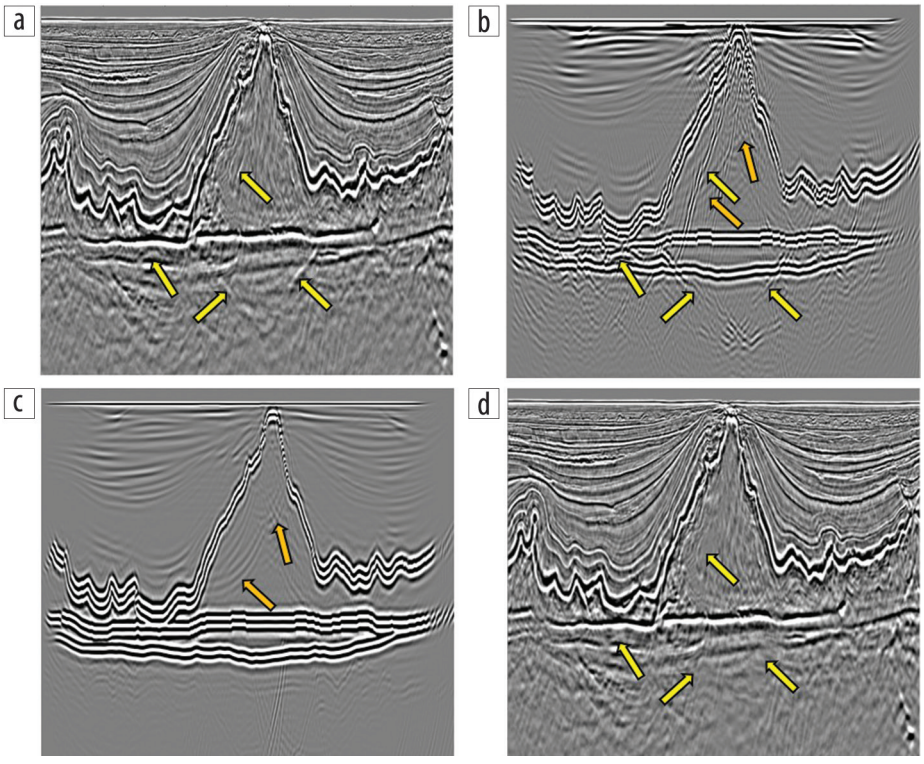

Figure 9. One line in a 3D RTM image volume from Campos Basin: (a) the original image, where converted wave images seriously contaminate the image of the base of salt and below; (b) P-wave RTM image of elastically simulated shot gathers; (c) P-wave RTM image of acoustically simulated shot gathers; and (d) the RTM image after adaptively subtracting the images of the predicted converted waves at the salt boundaries.

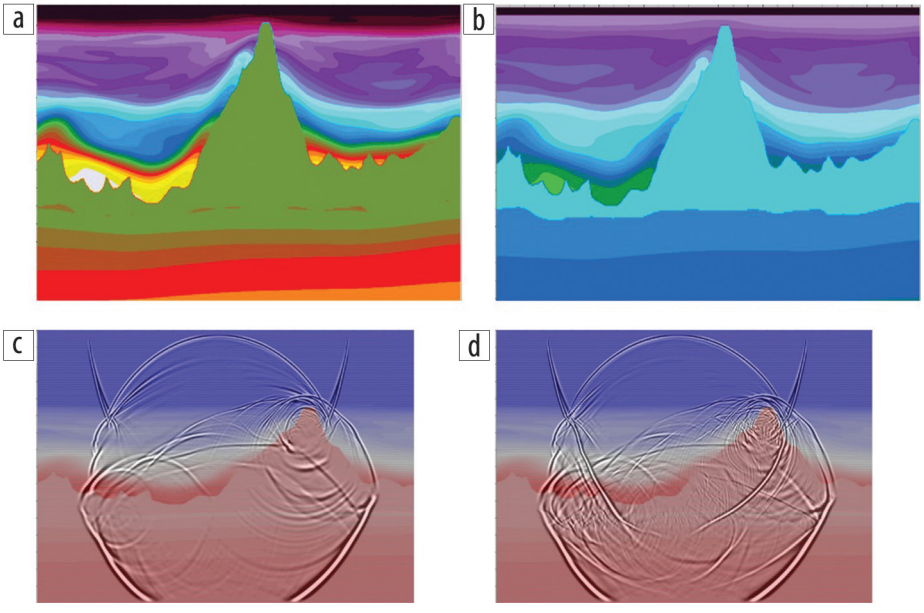

Figure 10. (a) A 2D section of the final P-wave velocity model. (b) S-wave velocity modified from the P-wave velocity between the water bottom and base of salt. (c) Wavefield snapshot of acoustic wave propagation. (d) Wavefield snapshot of elastic wave propagation.

density models using two-way wavefield extrapolation algorithms. The generation of pseudo VSP data has proved useful in understanding primaries, multiples, or mode-converted reflections through integration of unmigrated and migrated data. The pseudo VSP data section allows viewing the relation and propagation paths between events in the original shot gathers and the migrated sections (Alai and Wapenaar, 1994). For detailed information on improved predrilling views by pseudo seismic borehole data, the reader is referred to Alai (1997).

Pseudo VSP data via MDR and MME. The MME method of Zhang et al. (2019) is completely data driven and not dependent on any velocity model information (van der Neut and Wapenaar, 2016). MME retrieves shot records that only contain primary reflections. In addition, the Marchenko method can generate Green's functions of virtual receiver points in the subsurface in a correct two-way sense (Wapenaar et al., 2014; Brackenhoff et al., 2019), which we refer to as MDR. To compute the Green's function, the first arrival times, via a smooth data-estimated macromodel, from the virtual point to the surface are required. Displaying these Green's function results through a VSP configuration provides new insight on the handling of the interbed multiples. The Marchenko methods can attenuate interbed multiples (MME) or fully explain interbed multiples (MDR) in complex areas but require dense source and receiver sampling to achieve those results.

Pseudo VSP data via FWM. FWM was introduced by Berkhout (2014b). It is an inversion-based imaging method in which the up/downgoing wavefields are iteratively modeled in the medium and compared to the measured surface response. Its unique feature is that it uses the migration velocity model and the estimated reflectivities to recursively model primaries and all orders of (interbed) multiples. This process, called full-wavefield modeling (Berkhout 2014a), uses recursive one-way propagation and applies the boundary conditions at each depth level via the imaged reflectivities. By going up and down iteratively, the method iteratively models all scattered energy and includes accompanying transmission effects. As has been demonstrated by Davydenko and Verschuur (2017), this process reconstructs the up/downgoing wavefields at each depth level such that these wavefields can be displayed as snapshots or VSP-type recordings. In this way a fully image-consistent, two-way wavefield can be

reconstructed from the image and the background velocity model. Note again that all scattering is generated from the image that is extracted from the data. Also, because interbed multiples are explained during modeling, their crosstalk is fully removed from the image in the ideal scenario. Therefore, the FWM process can be called a model-assisted inversion approach: it relies to a large extent on the data but uses the physical relationships and the reflectivity image to build the wavefield at all depth levels. The upside of this approach is that FWM does not rely on fully sampled sources and receivers. As long as one of the two sides is well sampled, the imaging process takes care of creating physical consistency. Haffinger et al. (2017) described a target-oriented elastic inversion approach — based on the 1.5D version of the scattering integral — for which VSP-type displays can also be generated in the reservoir area under the local 1.5D assumption. Finally, note that Berkhout (2014a) also described the extension of FWM toward mode-converted waves, with initial results shown by Hoogerbrugge and Verschuur (2020). Such FWM extension could optimally combine images from both P-waves and mode-converted reflections into one integrated image, as already suggested by Alai and Verschuur (2006).

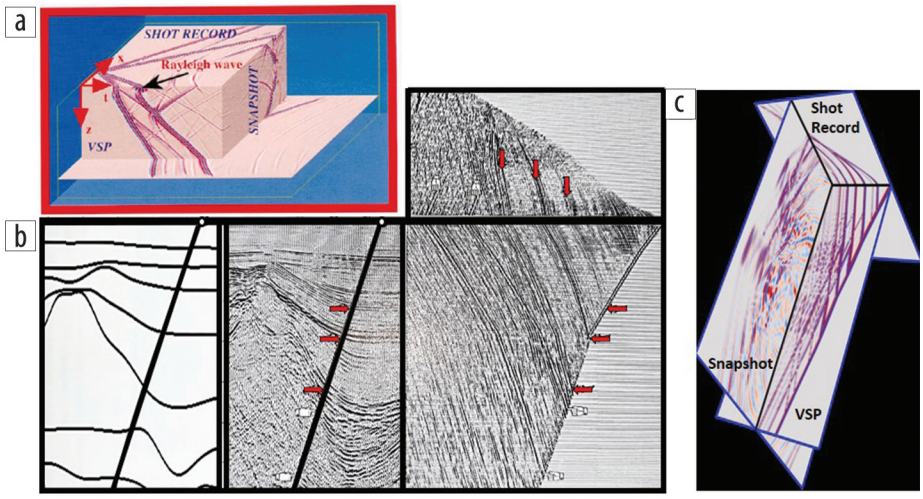

Figure 11. (a) 3D volume of elastic data illustrating the different cross sections, shot record, VSP, and snapshot (Alai and Wapenaar, 1993). (b) Integration of shot record, pseudo VSP, model, and PSDM (Alai, 1997). (c) 3D volume of data for the model in Figure 2 illustrating shot record, VSP, and snapshot.

Numerical data example of pseudo VSP generation

In the following, a numerical model has been designed to illustrate the advantages of generating pseudo VSP data using Marchenko methods, via MDR and MME, and FWM. The input data to these methods are generated by acoustic finite difference modeling. In Figure 11a, we show a 3D image of shot record, VSP, and snapshot (Alai and Wapenaar, 1993). In Figure 11b, an example of integration of shot record, pseudo VSP, model, and PSDM (Alai, 1997) is shown. Figure 11c shows a 3D image integrating a shot record, VSP, and snapshot for the model used in this paper. In Figure 12, we show the various (pseudo) VSP displays. An integrated display of zero-offset modeled VSP, subsurface model, and center shot record (primaries and interbed multiples only) is depicted in Figure 12a (right). In the left top row, we show the pseudo VSP for the MME output. Note that this pseudo VSP can be calculated with one-way wavefield propagation, such as used in Alai et al. (1995), and that the MME output is only computed from reflection data. Here, it is clearly visible where the primary reflections end up in the subsurface. In the middle panel we show the pseudo VSP-MDR result (Figure 12b, right), where the two-way wavefield is reconstructed without using accurate subsurface information. Note that now all multiple scattering is explained correctly. Such a display can help identify events observed in the surface data and relate them to either primaries or multiples. Note again that only densely sampled surface data and a smooth macromodel were used to generate all up/downgoing wavefields at depth. Note the clear definition of the primary reflection points. In the left panel, we used the primaries from MME (in blue) and the interbed multiples from MME (in red) and applied simple one-way back propagation, showing where interbed multiples (in red) will be wrongly mapped in depth.

For the third row in Figure 12, we applied FWM and generated the displayed FWM image and the reconstructed pseudo VSP data (Figure 12c, right). Again, we can use this display to analyze the observed events in the surface data. By switching off the interbed multiples and transmission effect generation in FWM, we actually perform standard least-squares migration (LSM), see Figure 12c (left). In this way, we treat all interbed multiples as primaries. This will result in a pseudo VSP display that does not provide much information to the user as all events are explained as if they were primary reflections. From Figure 12c, it is clearly observable that interbed multiples are suppressed from the FWM image as they are explained properly by the multiple scattering related to the image. The LSM pseudo VSP shows the well-known multiple crosstalk that may completely blur interpretation. Note also that in the deeper part, still not all multiple scattering is fully resolved, due to limited iterations. For the FWM/LSM results, shot records were used with a source sampling of only 160 m. This exercise allows MDR and FWM snapshots generation replacing finite difference snapshots, and their interpretation via pseudo VSP data.

Conclusions

In a geologic setting containing interfaces with large impedance contrast, such as salt or carbonate, strong mode conversion and interbed multiples can be generated at the interfaces. Images of these events can obscure the underneath structures and contaminate the image inside the salt body as well. The first part of this paper illustrates that it is critical to properly estimate these reflections and suppress them optimally. Cleaner subsalt sections should increase the confidence in identification of the deeper exploration opportunities and improve resolution of the highly heterogeneous subsalt carbonates. Increased signal-to-noise ratio, particularly for the subsalt reservoir section should allow more reliable amplitude-based seismic inversions. In addition, identification of the various

events will facilitate the path toward solutions. The generation of pseudo VSP from surface data was introduced as an interpretation tool that has proven to be useful in understanding primaries, multiples, or wave-converted reflections through integration and viewing events via unmigrated and migrated data. In the second part of this paper, we demonstrated via a salt-based example that with emerging full-wavefield methodologies, such as Marchenko-based methods and FWM, this old concept can be revived and can play a crucial role in better understanding the various waves propagating in the subsurface. TLE

Acknowledgments

We thank TGS Multiclient for permission to use the data examples. We are also grateful to Scott Michell for his guidance and encouragement as well as Sarah Spoors and James Sheng for their help. Furthermore, we would like to thank PETRONAS Carigali Sdn. Bhd. management for its support, guidance, and permissions to publish the results. Finally, we thank the sponsoring companies of the Delphi Consortium for their support.

Data and materials availability

Data associated with this research are confidential and cannot be released.

Corresponding author: riaz.alai@petronas.com

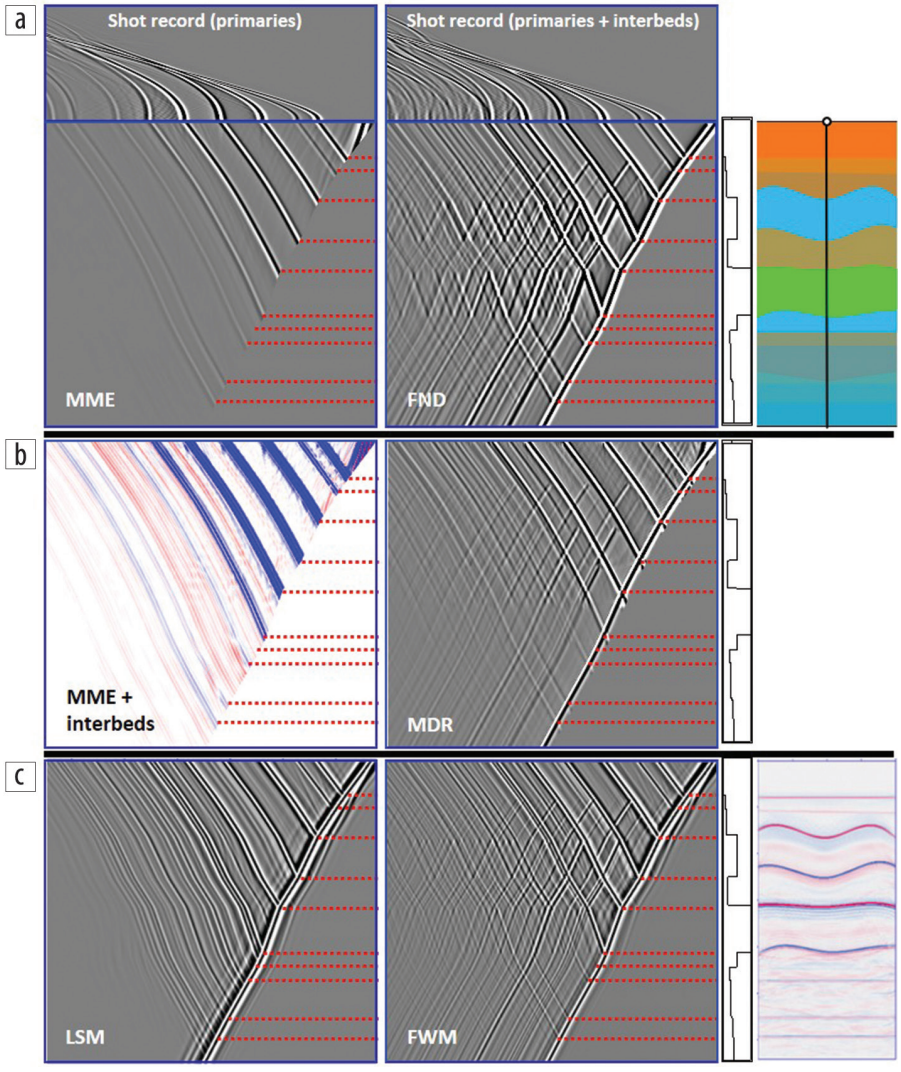

Figure 12. (a) [right] Integrated display of zero-offset modeled VSP, subsurface model, and center shot record (primaries and interbed only). [left] Integration of shot record (primaries only) and generated pseudo VSP for the MME output. Here, the MME was applied to suppress the interbed multiples, and this output was used to generate the pseudo VSP. (b) [left] In pseudo VSP generation, we used primaries from MME (in blue) and the interbed multiples from MME (in red) and applied simple one-way back propagation. It shows where interbed multiples, in red, will be wrongly mapped in depth. [right] Pseudo VSP-MDR result, where the two-way wavefield is reconstructed without using accurate subsurface information. Note that now all multiple scattering is explained correctly. Such displays can help identify events observed in the surface data and relate them to either primaries or multiples. (c) [right] FWM pseudo VSP and migration. It is clearly observable that interbed multiples are suppressed from the FWM image as they are explained properly by the multiple scattering related to the image. [left] LSM pseudo VSP.

References

Alai, R., and C. P. A. Wapenaar, 1993, Transformation of surface data into VSP data: 63rd Annual International Meeting, SEG, Expanded Abstracts, 143–146, https://doi.org/10.1190/1.1822420.

Alai, R., and C. P. A. Wapenaar, 1994, From seismic surface measurements to pseudo VSP data: 56th Conference and Exhibition, EAEG, Extended Abstracts, https://doi.org/10.3997/2214-4609.201409819.

Alai, R., W. E. A. Rietveld, C. P. A. Wapenaar, and A. J. Berkhout, 1995, From seismic surface measurements to pseudo VSP data: A new tool in 3-D seismic interpretation: 4th International Congress of the Brazilian Geophysical Society, Conference Proceedings, 451–455, https://doi.org/10.3997/2214-4609-pdb.313.137.

Alai, R., 1997, Improving predrilling views by pseudo seismic borehole data: PhD thesis, Delft University of Technology.

Alai, R., and D. J. Verschuur, 2003, Simultaneous adaptive least-squares subtraction of multiples: 65th Conference and Exhibition, EAGE, Extended Abstracts, https://doi.org/10.3997/2214-4609-pdb.6.P193.

Alai, R., and D. J. Verschuur, 2006, Subsalt imaging of wave converted reflections in physical model data: 68th Conference and Exhibition, EAGE, Extended Abstracts, https://doi.org/10.3997/2214-4609.201402156.

Alai, R., J. Thorbecke, and E. Verschuur, 2007, Subsalt illumination studies through longitudinal and transversal wave propagation: 10th International Congress of the Brazilian Geophysical Society, Conference Proceedings, https://doi.org/10.3997/2214-4609-pdb.172.SBGF0286_07.

Berkhout, A. J., 2014a, Review paper: An outlook on the future of seismic imaging, Part I: Forward and reverse modelling: Geophysical Prospecting, **62**, no. 5, 911–930, https://doi.org/10.1111/1365-2478.12161.

Berkhout, A. J., 2014b, Review paper: An outlook on the future of seismic imaging, Part II: Full wavefield migration: Geophysical Prospecting, **62**, no. 5, 931–949, https://doi.org/10.1111/1365-2478.12154.

Brackenhoff, J., J. Thorbecke, and K. Wapenaar, 2019, Virtual sources and receivers in the real earth: Considerations for practical applications: Journal of Geophysical Research: Solid Earth, **124**, no. 11, 11,802–11,821, https://doi.org/10.1029/2019JB018485.

Chang, S. G., B. Yu, and M. Vetterli, 2000, Adaptive wavelet thresholding for image denoising and compression: IEEE Transactions on Image Processing, **9**, no. 9, 1532–1546, https://doi.org/10.1109/83.862633.

DOI:10.1190/tle40120905.1

Davydenko, M., and D. J. Verschuur, 2017, Full-wavefield migration: Using surface and internal multiples in imaging: Geophysical Prospecting, **65**, no. 1, 7–21, https://doi.org/10.1111/1365-2478.12360.

Griffiths, M., J. Hembd, and H. Prigent, 2011, Applications of interbed multiple attenuation: The Leading Edge, **30**, no. 8, 906–912, https://doi.org/10.1190/1.3626498.

Haffinger, P., F. J. Eyvazi, P. Doulgeris, P. Steeghs, D. Gisolf, and E. Verschuur, 2017, Quantitative prediction of injected CO_2 at Sleipner using wave-equation based AVO: First Break, **35**, no. 7, https://doi.org/10.3997/1365-2397.35.7.89731.

Hegazy, M., A. Stewart, S. Hydal, K. Malave, and O. Mataracioglu, 2017, Salt-related converted-wave attenuation: A Gulf of Mexico example: 87th Annual International Meeting, SEG, Expanded Abstracts, 4609–4613, https://doi.org/10.1190/segam2017-17494947.1.

Hoogerbrugge, L., and E. Verschuur, 2020, Including converted waves in full wavefield migration: 82nd Conference and Exhibition, EAGE, Extended Abstracts, https://doi.org/10.3997/2214-4609.202011693.

Huang, Y., W. Gou, O. Leblanc, Y. Li, S. Ji, and Y. Huang, 2013, Study and application of salt-related converted waves in imaging: 83rd Annual International Meeting, SEG, Expanded Abstracts, 3851–3855, https://doi.org/10.1190/segam2013-1291.1.

Jakubowicz, H., 1998, Wave equation prediction and removal of interbed multiples: 68th Annual International Meeting, SEG, Expanded Abstracts, 1527–1530, https://doi.org/10.1190/1.1820204

Lu, R. S., D. E. Willen, and I. A. Watson, 2003, Identifying, removing and imaging P-S conversions at salt-sediment interfaces: Geophysics, **68**, no. 3, 1052–1059, https://doi.org/10.1190/1.1581076.

Penna, R., G. Camargo, P. R. Johann, and R. Dias, 2013, Challenges in seismic imaging and reservoir characterization of presalt oilfields in offshore Brazil: Offshore Technology Conference, OTC-24173-MS, https://doi.org/10.4043/24173-MS.

Pereira, R., D. Mondini, and D. Donno, 2018, Efficient 3D internal multiple attenuation in the Santos Basin: Conference Proceedings, 80th Conference and Exhibition, EAGE, Extended Abstracts, https://doi.org/10.3997/2214-4609.201801073.

Staring, M., and K. Wapenaar, 2020, Three-dimensional Marchenko internal multiple attenuation on narrow azimuth streamer data of the Santos Basin, Brazil: Geophysical Prospecting, **68**, no. 6, 1864–1877, https://doi.org/10.1111/1365-2478.12964.

Tang, C., Y. He, J. Mao, and J. Sheng, 2019, Fourier finite-difference wave-equation migration in tilted transversely isotropic media with an improved solution for coefficient estimation: 89th Annual International Meeting, SEG, Expanded Abstracts, 4292–4296, https://doi.org/10.1190/segam2019-3214439.1.

Van der Neut, J., and K. Wapenaar, 2016, Adaptive overburden elimination with the multidimensional Marchenko equation: Geophysics, **81**, no. 5, T265–T284, https://doi.org/10.1190/geo2016-0024.1.

Wang, B., M. Guo, C. Mason, J. Cai, S. Gajawada, and D. Epili, 2009, Wave-equation based residual multiple prediction and elimination in migration depth domain as an aid to seismic interpretation: 79th Annual International Meeting, SEG, Expanded Abstracts, 3123–3127, https://doi.org/10.1190/1.3255505.

Wapenaar, K., J. Thorbecke, J. Van der Neut, F. Broggini, E. Slob, and R. Snieder, 2014, Marchenko imaging: Geophysics, **79**, no. 3, WA39–WA57, https://doi.org/10.1190/geo2013-0302.1.

Weglein, A. B., F. A. Gasparotto, P. M. Carvalho, and R. H. Stolt, 1997, An inverse scattering series method for attenuating multiples in seismic reflection data: Geophysics, **62**, no. 6, 1975–1989, https://doi.org/10.1190/1.1444298.

Xavier de Melo, F., M. F. Pantoja, M. Ortin, and E. Medina, 2020, Optimized 3D and true-azimuth internal multiple attenuation strategy in the Santos Basin: 90th Annual International Meeting, SEG, Expanded Abstracts, 3214–3218, https://doi.org/10.1190/segam2020-3428310.1.

Yang, C., Y. Huang, Z. Liu, J. Sheng, and E. Camarda, 2020, Shear wave noise attenuation and wavefield separation in curvelet domain: 90th Annual International Meeting, SEG, Expanded Abstracts, 1805–1809, https://doi.org/10.1190/segam2020-3426418.1.

Zhang, L., J. Thorbecke, K. Wapenaar, and E. Slob, 2019, Transmission compensated primary reflection retrieval in the data domain and consequences for imaging: Geophysics, **84**, no. 4, Q27–Q36, https://doi.org/10.1190/geo2018-0340.1.